Momentum distribution of helium and hydrogen in nanotubes

S. M. Gatica,[1,2] M. W. Cole,[1,*] G. Stan,[1,†] J. M. Hartman,[1] and V. H. Crespi[1]
[1]*Department of Physics, Penn State University, University Park, Pennsylvania 16802*
[2]*Departamento de Física, Facultad de Ciencias Exactas y Naturales, Universidad de Buenos Aires, Ciudad Universitaria, RA-1428 Buenos Aires, Argentina*
(Received 6 June 2000)

We compute the momentum distribution of helium atoms and hydrogen molecules absorbed within an ordered bundle of carbon nanotubes. The results vary significantly as a function of coverage and manifest the strong anisotropy and localization of this geometry. For example, the root-mean-square momentum component perpendicular to the bundle axis can be about three times larger for interstitial molecules than for molecules moving in an axial phase confined by a cylindrical film of particles coating the tube's inner wall. These results (which are consequences of the uncertainty principle) indicate that the momentum distribution is a useful signature of the local geometry and quantum state of the absorbed particles in nanotube bundles.

Much interest has been attracted to the problem of gases absorbed within carbon nanotubes,[1–11] motivated by both fundamental physics and the potential for application in gas storage, separation, and sensing. Experimental evidence suggests that quantum gases like helium and hydrogen could be especially strongly absorbed in this environment.[1,2,5,12,13] Theoretical calculations of several groups have also found the adsorption potential to be highly attractive for small atoms and molecules due to the high coordination in the curved environment.[13,14] The properties of this adsorbate are of fundamental interest because of the reduced dimensionality they manifest.[15,16] One of the many techniques suitable for characterizing adsorbed particles is neutron scattering.[17–23] For a high surface area material, such scattering data (elastic or inelastic, coherent or incoherent) can provide information about the static (e.g., ordered structural) and dynamic (e.g., diffusive) properties. In this paper, we compute the momentum distribution, which is probed by incoherent inelastic neutron scattering. We find this to be a sensitive probe of the state of the adsorbate, enabling one to distinguish between alternative adsorption locations and configurations. This discrimination can be quite valuable because other kinds of experimental information (e.g., thermodynamics) tend to provide complementary information (e.g., about structure or energy).

When ordered bundles of clean, opened carbon nanotubes are exposed to a helium or hydrogen vapor, it is expected that adsorption occurs in both the interstitial channels and within the tubes.[12] Inside the tubes, the particles first coat the tube's inner wall, forming a cylindrical shell-gas phase.[14,24] As the density of the inner atoms or molecules increases beyond a certain value, the film will solidify, with the particles localized in a cylindrical lattice (shell-localized phase). For sufficiently high chemical potential (or pressure), the region in the center of the tube starts to become populated, forming an axial phase.[24] We calculate the momentum distribution of the four different phases mentioned above, i.e., the interstitial-channel phase, the shell-gas phase, the shell-localized phase, and the axial phase. The contribution of each phase to the total momentum distribution is proportional to the number of particles in each phase. Reference 24 discusses the coverage as a function of the thermodynamic variables. Here we assume that the temperature is zero, i.e. each phase is in its ground state. Of the four phases discussed here, only the shell-localized phase manifests correlations between the adsorbed particles. The other phases exhibit distinctive effects of the confinement by the host.

To compute the momentum distribution of one single particle, we Fourier-transform the single-particle wave function $\psi(\vec{\mathbf{r}})$,

$$a(\vec{\mathbf{k}}) = \frac{1}{(2\pi)^{3/2}} \int d\vec{\mathbf{r}} e^{-i\vec{\mathbf{k}}\cdot\vec{\mathbf{r}}} \psi(\vec{\mathbf{r}}). \tag{1}$$

The occupation number of momentum states is $n(\vec{\mathbf{k}}) = |a(\vec{\mathbf{k}})|^2$.

We first focus our attention on the distribution of momentum perpendicular to the axis (z) of the nanotube,

$$n(\vec{K}) = \int dk_z \, n(\vec{\mathbf{k}}), \tag{2}$$

where $\vec{K} = (k_x, k_y)$. If the wave function is cylindrically symmetric, i.e., $\psi(\vec{\mathbf{r}})$ depends only on the distance r to the axis, then $n(\vec{K}) \equiv n(K) = |a(K)|^2$, $(K = |\vec{K}|)$ where

$$a(K) = \int_0^\infty r \, dr \, \psi(r) \, J_0(Kr). \tag{3}$$

The number of particles per unit increment dK in an interval $[K, K+dK]$ is $N(K) = 2\pi K \, n(K)$ in an azimuthally isotropic situation. This applies to the axial phase, the shell-gas phase, and the interstitial-channel phase, if we neglect the anisotropy. Here we show that the momentum distributions of the four phases are distinguishable from the different widths in momentum space. The single-particle wave functions $\psi(r)$ needed for the calculation of the $a(K)$ were taken from Ref. 24 for the axial and shell phases, and from Ref. 25 for the interstitial channel.

In the case of the shell-localized phase, the adsorbate's mutual interaction changes the situation significantly. Al-

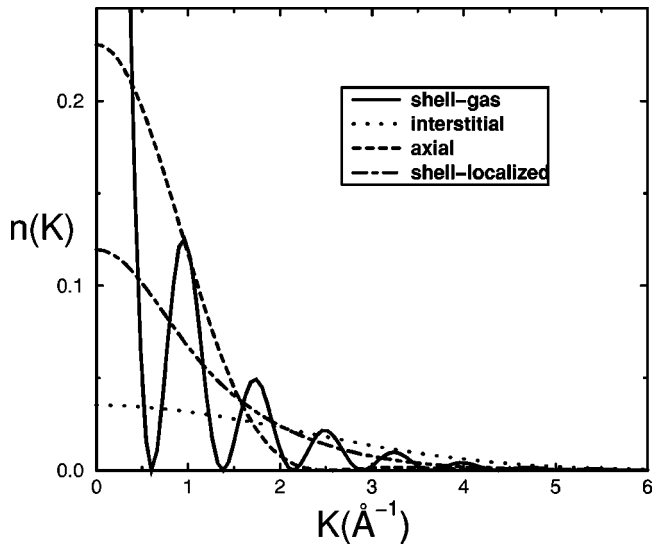

FIG. 1. Momentum distribution $n(K)$ for ^{4}He, for the four phases mentioned in the text.

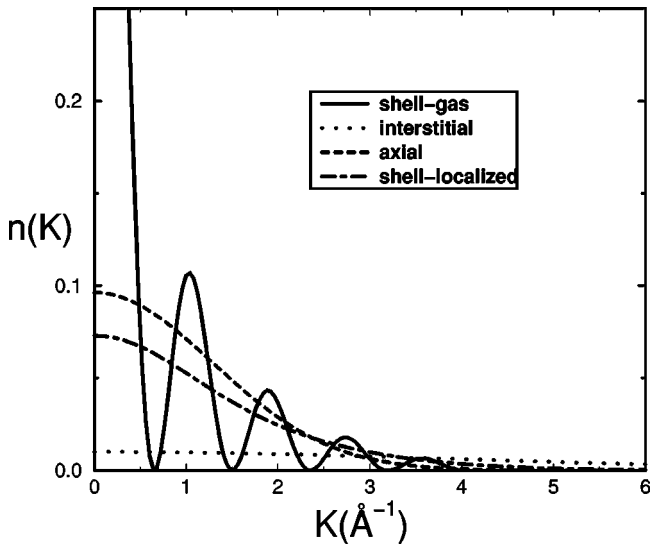

FIG. 2. The same as Fig. 1 for H_2.

though there is no experimental evidence concerning the structure of this phase, we assume for our calculations that the equilibrium configuration is that of a monolayer above flat graphite that has been rolled up, forming a cylindrical shell. The radius (R) and thickness (δR) of the shell are, respectively, the mean values $\langle r\rangle$ and $\langle (r^2-\langle r\rangle^2\rangle^{1/2}$, determined by our previous calculations of the single-particle wave function $\psi(\vec{r})$ of ^{4}He or H_2 inside a nanotube.[24] For a nanotube with a diameter of 14 Å, $R=4.07$ Å and $\delta R=0.27$ Å for ^{4}He, and $R=3.63$ Å and $\delta R=0.23$ Å for H_2. With these considerations in mind, we calculate the momentum distribution in the following way. Let $N_{\rm local}(k_r,k_\phi,k_z)$ be the momentum distribution of one particle localized in a particular position in the shell, characterized by its cylindrical coordinates (R,ϕ,z). Then we evaluate the momentum distribution $N(k)$ as the integral

$$N(k)=\int d\phi \int dk_r\, dk_\phi\, dk_z\, N_{\rm local}(k_r,k_\phi,k_z) \times \delta(k-\sqrt{k_r^2+k_\phi^2}). \tag{4}$$

The delta function selects those particles with the appropriate momentum. We assume that the function $N_{\rm local}(k_r,k_\phi,k_z)$ is a product of three Gaussians, as determined from *ab initio* calculations.

$$N_{\rm local}(k_r,k_\phi,k_z)=\frac{\sqrt{\delta\gamma^2}}{\pi^{3/2}} e^{-\delta k_r^2} e^{-\gamma k_\phi^2} e^{-\gamma k_z^2}. \tag{5}$$

The values of δ and γ are calculated by Fourier transforming the corresponding local single-particle wave function $\psi(r)$, being $\delta=0.16$ Å^2 for ^{4}He, and $\delta=0.11$ Å^2 for H_2. The value of γ comes from the Fourier transform of the wave function above flat graphite, which can be found in the literature[26,27] and that depends on θ. For ^{4}He, γ varies from 0.7 to 1.63 Å^2 for $\theta=0.0995$ to 0.07 Å^{-2},[26] while for H_2 we take $\gamma=0.73$ Å^2, corresponding to $\theta=0.085$ Å^{-2}.[27]

The results are shown in Figs. 1 and 2 for ^{4}He and H_2, respectively, where we plot the function $n(k)$ for each phase. The momentum distribution in the interstices is the broadest, as expected due to the high confinement in real space, followed by the shell-localized, shell-gas, and axial phases. Notice that the shell-gas phase shows rings as a consequence of the confinement of the ground-state wave function far from and homogeneously around the axis. The rings are evident from Eq. (3) in the limiting case when $\psi(r)\sim\delta(r-R)$ so that $a(K)\sim RJ_0(KR)$. The oscillations are lost when the density of the shell increases and the localized phase replaces the gas phase. Table I gives the mean square values of the momentum $k_{\rm rms}=\sqrt{\langle k_x^2\rangle}$. For H_2, the state dependence is most dramatic; $k_{\rm rms}$ for the interstitial phase is more than three times that for the shell gas. In the shell-localized phase, $k_{\rm rms}$ varies with the shell density θ in the form,

$$\langle k_x^2\rangle_{\text{shell-loc}}(\theta)=\frac{1}{4\delta}+\frac{1}{4\gamma(\theta)}. \tag{6}$$

as derived from Eqs. (4) and (5).

Regarding the momentum distribution in the z direction, we evaluated the function $n(k_z)$, for the shell-localized and interstitial phases [the axial and shell-gas phases are homogeneous in the z direction, consequently $n(k_z)\sim\delta(k_z)$]. For the shell-localized phase, the mean- square momentum is $\langle k_z^2\rangle=1/2\ \gamma(\theta)$, whose values are presented in Table I. Notice that these mean values are lower than the corresponding

TABLE I. Root-mean-square momentum perpendicular (parallel) to the tube axis, $\sqrt{\langle k_x^2\rangle}$ ($\sqrt{\langle k_z^2\rangle}$), in Å^{-1} corresponding to the different phases.

Phase	^{4}He	H_2
Interstitial	2.07 (1.41)	3.94
Shell localized	1.31 (0.55)*	1.62 (0.83)
Shell gas	1.19	1.22
Axial	0.86	1.28

* For $\theta=0.07$ Å^{-2}

values in the x direction, reflecting the smaller width of the shell. For the interstitial phase of Ref. 25 we find that $\sqrt{\langle k_z^2\rangle}=1.41$ Å^{-1} for ^{4}He.

We turn briefly to the effect of temperature $T\equiv(k_B\beta)^{-1}$ for the interstitial gas. For finite T the momentum distribution is calculated by integrating over the Boltzmann-weighted distribution of axial wave vectors k (in the classical-statistics density regime),

$$n(k_z)=\frac{\int dk\, e^{-\beta E(k)}\, n(k_z;k)}{\int dk\, e^{-\beta E(k)}}, \tag{7}$$

and the mean value reads

$$\langle k_z^2\rangle=\frac{\int dk\, e^{-\beta E(k)}\langle k_z^2\rangle_k}{\int dk\, e^{-\beta E(k)}}. \tag{8}$$

For ^{4}He in an ordered aligned bundle of (18,0) nanotubes, the band energy $E(k)$ is centered around ~ -370 K with a narrow bandwidth of ~ 0.2 K.[25] The mean values of $\sqrt{\langle k_z^2\rangle}$ are 1.415 Å^{-1} and 1.406 Å^{-1} for $k=0$ and π/a, respectively, so the temperature does not significantly affect this calculation so long as higher bands (separated by ~ 10 K but dependent on the detailed tube wrapping angles and relative orientations, with some cases yielding axially incommensurate structures) are not occupied. These values correspond to axis-parallel kinetic energies $E_z\sim 11$ K. The high energy (like the narrow band width) is a consequence of the highly corrugated potential along the interstitial channel for this bundle geometry. Note that the single-particle axial absorbate band structure could be sensitive to variations in tube wrapping angles and relative orientations, and interparticle interactions could become important at higher coverages, partcularly in certain geometries.

In a situation where adsorption occurs in all sites inside and between tubes, the total momentum distribution would be a weighted sum of the four contributions,

$$N_{\text{total}}(k)=A_{\text{inter}}N_{\text{inter}}+A_{\text{shell-gas}}N_{\text{shell-gas}}+A_{\text{shell-loc}}N_{\text{shell-loc}}+A_{\text{axial}}N_{\text{axial}}. \tag{9}$$

The weight factors $A_{\ldots}$ depend on the particle distribution and hence the chemical potential. For the tube geometries studied, the first contribution to appear is $A_{\text{inter}}N_{\text{inter}}(k)$. The next is the shell-gas term, making rings in the momentum distribution. As the coverage increases, $A_{\text{shell-gas}}$ goes to zero, and the localized term $A_{\text{shell-loc}}N_{\text{shell-loc}}(k)$ replaces it, washing out the rings. Finally, the last term would add a low-momentum contribution. If some of the sites were excluded, for instance if the tubes are closed, that would be revealed by the absence of the corresponding term in the momentum distribution.

We are grateful to Michel Bienfait and Paul Sokol for helpful discussions. This research was supported by the National Science Foundation through Grant Nos. DMR-9705270 and DMR-9876232, the Petroleum Research Fund of the American Chemical Society through Grant No. PRF 33824-G5 and Grant No. PRF 34308-AC5 and the Army Research Office Grant No. DAAD19-99-1-0167.

*Corresponding author. Email: mwc@psu.edu, FAX: 814-865-3604.

†Present address: Institute for Physical Science and Technology and Department of Chemical Engineering, University of Maryland, College Park, Maryland 20742.

[1] A.C. Dillon, K.M. Jones, T.A. Bekkedahl, C.H. Kiang, D.S. Bethune, and M.J. Heben, Nature (London) **386**, 377 (1997).

[2] K.A. Williams and P.C. Eklund, Chem. Phys. Lett. **320**, 352 (2000).

[3] A. Chambers, C. Park, R.T.K. Baker, and N.M. Rodriguez, J. Phys. Chem. B **102**, 4253 (1998).

[4] S. Inoue, N. Ichikuni, T. Suzuki, T. Uematsu, and K. Kaneko, J. Phys. Chem. B **102**, 4689 (1998).

[5] W. Teizer, R.B. Hallock, E. Dujardin, and T.W. Ebbesen, Phys. Rev. Lett. **82**, 5305 (1999); erratum **84**, 1844 (2000).

[6] C. Nützenadel, A. Züttel, D. Chartouni, and L. Schlapbach, Electrochem. Solid-State Lett. **2**, 30 (1999).

[7] S. Orimo, G. Majer, T. Fukunaga, A. Züttel, L. Schlapbach, and H. Fujii, Appl. Phys. Lett. **75**, 3093 (1999).

[8] E.B. Mackie, R.A. Wolfson, L.M. Arnold, K. Lafdi, and A.D. Migone, Langmuir **13**, 7197 (1997); S. Weber, S. Talapatra, C. Journet, and A.D. Migone, Phys. Rev. B **61**, 13150 (2000).

[9] A. Kuznetsova, J.T. Yates, Jr., J. Liu, and R.E. Smalley, J. Chem. Phys. **112**, 9590 (2000).

[10] Y. Ye, C.C. Ahn, C. Witham, B. Fultz, J. Liu, A.G. Rinzler, D. Colbert, K.A. Smith, and R.E. Smalley, Appl. Phys. Lett. **74**, 2307 (1999).

[11] P. Chen, X. Wu, J. Lin, and K.L. Tan, Science **285**, 91 (1999); Q. Wang and J.K. Johnson, J. Chem. Phys. **110**, 577 (1999).

[12] G. Stan, M.J. Bojan, S. Curtarolo, S.M. Gatica, and M.W. Cole, Phys. Rev. B **62**, 2173 (2000).

[13] Q. Wang and J.K. Johnson, J. Phys. Chem. B **103**, 277 (1999).

[14] G. Stan and M.W. Cole, J. Low Temp. Phys. **110**, 539 (1998).

[15] A.M. Vidales, V.H. Crespi, and M.W. Cole, Phys. Rev. B **58**, R13 426 (1998).

[16] M.W. Cole, V.H. Crespi, G. Stan, C.A. Ebner, J.M. Hartman, S. Moroni, and M. Boninsegni, Phys. Rev. Lett. **84**, 3883 (2000).

[17] *Momentum Distributions*, edited by R. N. Silver and P. E. Sokol (Plenum, New York, 1990).

[18] H. Fu, F. Trouw, and P.E. Sokol, J. Low Temp. **116**, 149 (1999).

[19] D.W. Brown, P.E. Sokol, and S.A. FitzGerald, Phys. Rev. B **59**, 13 258 (1999).

[20] R.M. Dimeo, P.E. Sokol, R.T. Azuah, S.M. Bennington, W.G. Stirling, and K. Guckelsberger, Physica B **241**, 952 (1997).

[21] H.R. Glyde, Phys. Rev. B **50**, 6726 (1994).

[22] P.C. Hohenberg and P.M. Platzman, Phys. Rev. **152**, 198 (1966).

[23] M. Bienfait, in *Dynamics of Molecular Crystals*, edited by J. Lascombe (Elsevier, Amsterdam, 1987) pp. 353-63.

[24] S.M. Gatica, G. Stan, M.M. Calbi, J.K. Johnson, and M.W. Cole, J. Low Temp. Phys. (to be published).

[25] J.M. Hartman and V.H. Crespi (unpublished).

[26] P.A. Whitlock, G.V. Chester, and B. Krishnamachari, Phys. Rev. B **58**, 8704 (1998).

[27] X.-Z. Ni and L.W. Bruch, Phys. Rev. B **33**, 4584 (1986).